version1.4

arXiv:1111.6213v2 [nucl-th] 13 Jan 2012

Study of triangular flow v_3 in Au+Au and Cu+Cu collisions with a multiphase transport model

Kai Xiao,[1, 2] Na Li,[3, *] Shusu Shi,[1, 2, †] and Feng Liu[1, 2]
[1] *Institute of Particle Physics, Central China Normal University, Wuhan, Hubei, 430079, China*
[2] *The Key Laboratory of Quark and Lepton Physics (Central China Normal University), Ministry of Education, Wuhan, Hubei, 430079, China*
[3] *Department of Physics, Huazhong University of Science and Technology, Wuhan 430074, China*

(Dated: January 16, 2012)

We studied the relation between the initial geometry anisotropy and the anisotropic flow in a multiphase transport model (AMPT) for both Au+Au and Cu+Cu collisions at $\sqrt{s_{NN}}$=200 GeV. It is found that unlike the elliptic flow v_2, little centrality dependence of the triangular flow v_3 is observed. After removing the initial geometry effect, v_3/ε_3 increases with the transverse particle density, which is similar to v_2/ε_2. The transverse momentum (p_T) dependence of v_3 from identified particles is qualitatively similar to the p_T dependence of v_2.

PACS numbers: 25.75.Ld, 25.75.Dw

I. INTRODUCTION

A novel state of matter called quark-gluon plasma (QGP) composed by deconfined partons is believed to be created experimentally in heavy ion collisions at RHIC [1]. The discovery of large elliptic flow indicates that the partonic collectivity is built up during the collisions, and the number-of-quark scaling suggests that the partonic degrees of freedom are active [2].

The anisotropic flow is usually described by a Fourier decomposition of the azimuthal distribution with respect to the reaction plane [3]. The second harmonic coefficient, v_2, so called elliptic flow, has the biggest magnitude at high energy collisions [4]. It is believed that the observed anisotropy in the momentum space is caused by the anisotropy in the coordinate space in the initial condition. Lots of attention has been put on the relation between v_2 and spatial eccentricity to see the hydrodynamics behavior of the created system [5–7].

Recent studies show that the event-by-event fluctuation of the initial geometry [8] may play an important role in the study of collective flow. The triangular shape in the initial geometry will be transferred to the momentum space as the system expands, and finally leads to the none zero value of the third harmonic coefficient, v_3. It is found that the triangular flow v_3 is responsible for the ridge and shoulder structures and the broad away-side of two-particle azimuthal correlation [9]. Besides, it is also considered to be a good probe to study the viscous hydrodynamics behavior of the colliding system [10].

Lots of properties of the triangular flow v_3 have been studied in hydrodynamic and transport models [10, 11]. However, since the reaction plane can not be directly measured in the experiment, those anisotropic parameters can not be directly obtained. It is found that different methods may cause up to 20% discrepancy on v_2 [16], thus it should also be carefully evaluated for the v_3 study. Besides, v_3 is directly related with the initial fluctuation, it is interesting to see its system size dependence.

In this paper, we will study the triangular flow v_3 in both Au+Au and Cu+Cu collisions in a multiphase transport model (AMPT) [12]. The relation between v_3 and ε_3 is studied as a function of number of participants and transverse momentum. The paper is organized as follows: In Sec. II, the observables and technical methods are introduced. A brief description of AMPT model is given in Sec. III. The results and discussions are presented in Sec. IV. Finally, a summary is given in Sec. V.

II. OBSERVABLES

In a non-central collisions, the overlap region of two nuclei is an almond shape. Since the position of nucleons may fluctuate event by event, as discussed in Ref [13–15], those initial geometric irregularities of the colliding system can be described by ε_n:

$$\varepsilon_n = \frac{\sqrt{\langle r^2 \cos(n\varphi)\rangle^2 + \langle r^2 \sin(n\varphi)\rangle^2}}{\langle r^2 \rangle}, \tag{1}$$

where r and φ are the polar coordinate position of participating nucleons and $\langle \cdots \rangle$ is the average over all the participants in an event. n refers to the n-th harmonic, i.e., ε_2 describes the elliptic shape and ε_3 describes the triangular shape.

As the system evolves, the anisotropy in the coordinate space is transferred to the anisotropy in the momentum space due to the pressure gradient. The particle distri-

---

[*] Electronic address: nli@mail.hust.edu.cn
[†] Electronic address: sss@iopp.ccnu.edu.cn

bution then can be written as

$$\frac{dN}{d\phi} \propto 1 + 2\sum_{n=1} v_n \cos[n(\phi - \Psi_n)], \tag{2}$$

where ϕ is the azimuthal angle, and Ψ_n is the n-th event plane angle reconstructed by the final state particles:

$$\Psi_n = \frac{1}{n}\left[\tan^{-1}\frac{\sum\limits_i \sin(n\phi_i)}{\sum\limits_i \cos(n\phi_i)}\right]. \tag{3}$$

The observed anisotropic flow is defined as the n-th Flourier coefficient v_n:

$$v_n^{\mathrm{obs}} = \langle\cos[n(\phi - \Psi_n)]\rangle\,. \tag{4}$$

Here $\langle\cdots\rangle$ is taking the average over all the particles in the sample.

This is the so-called event plane method of calculating v_n. The reconstructed event plane fluctuates around the reaction plane. The observed signals need to be revised by the corresponding resolution [3]:

$$v_n = \frac{v_n^{\mathrm{obs}}}{\mathscr{R}_n}. \tag{5}$$

Due to the finite multiplicity of final state particles, the resolution

$$\mathscr{R}_n = \langle\cos[n(\Psi_n - \Psi_{\mathrm{nR}})]\rangle \tag{6}$$

is usually smaller than 1. Ψ_{nR} represents the nth real event plane angle.

III. AMPT MODEL

There are four main components in AMPT model: the initial conditions, parton interactions, hadronization and hadron interactions. The initial conditions are obtained from the HIJING model [17], which includes the spatial and momentum distributions of minijet partons from hard processes and strings from soft processes. The time evolution of partons is then treated according to the ZPC [18] parton cascade model. After partons stop interacting, a combined coalescence and string fragmentation model are used for the hadronization of partons. The scattering among the resulting hadrons is described by a relativistic transport (ART) model [19] which includes baryon-baryon, baryon-meson and meson-meson elastic and inelastic scattering.

In our study, we analyzed the events from AMPT with the parton cross section equals to 3 mb and 10 mb. As all the conclusions are independent on the parton cross section, only the results from 3 mb are shown in this paper. There are about 8 million events in Au + Au collisions and 19 million events in Cu+Cu collisions at $\sqrt{s_{NN}}$= 200 used. The string melting AMPT version is used since the previous study shows that the string melting AMPT version agrees with the experimental results better [12]. The centrality is defined by the impact parameter.

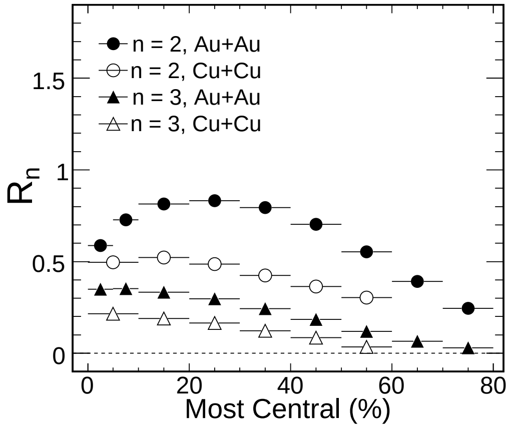

FIG. 1: The second and third harmonic event plane resolution calculated by the particles with pseudo-rapidty region of $|\eta| > 2$ as a function of centrality in both Au+Au and Cu+Cu collisions at $\sqrt{s_{NN}}$=200 GeV in AMPT model.

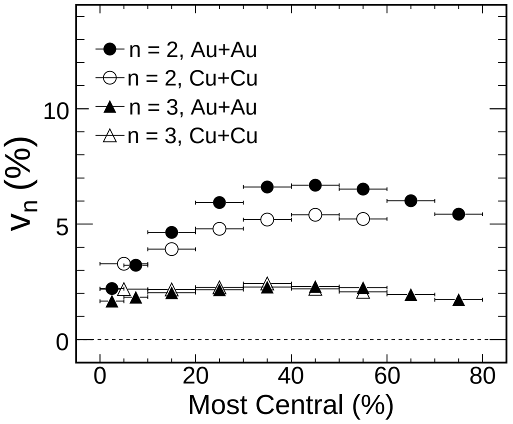

FIG. 2: v_n as a function of centrality in both Au+Au and Cu+Cu collisions at $\sqrt{s_{NN}}$=200 GeV in AMPT model.

IV. RESULTS AND DISCUSSIONS

In order to be comparable with the experimental data, the event plane method is used to calculate v_n. The procedure is slightly different between ours and Ref. [11], in which the event plane was reconstructed by initial partons. Charged particles with $p_T \leq 2$ GeV/c, $|\eta| > 2$ are chosen to reconstruct the event plane according to the Eq. 3. The particles used for the v_n measurements are within the $|\eta| < 1$. The η gap used here is to reduce the auto-correlation between the particles used to reconstruct the event plane and the particles of interest. In the following, the observed v_n are all corrected by the corre-

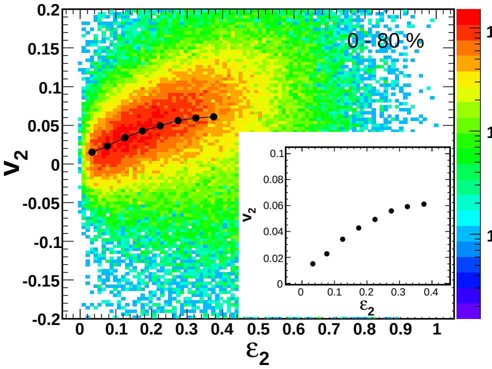

FIG. 3: (Color online) v_2 as a function of ε_2 in Au+Au collisions at $\sqrt{s_{NN}}$=200 GeV in AMPT model. The black points are the average v_2 in the selected ε_2 bin. The pad in the right down corner is the average of v_2 with smaller scale.

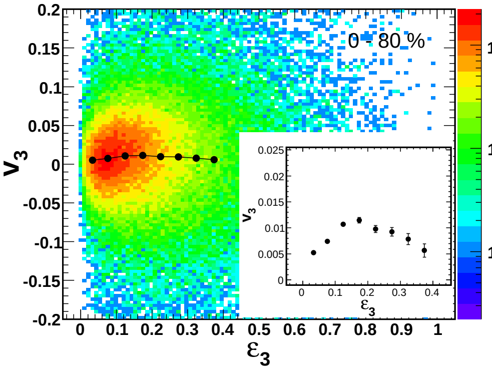

FIG. 4: (Color online) v_3 as a function of ε_3 in Au+Au collisions at $\sqrt{s_{NN}}$=200 GeV in AMPT model. The black points are the average v_3 in the selected ε_3 bin. The pad in the right down corner is the average of v_3 with smaller scale.

sponding resolution. Fig. 1 shows the resolution of v_2 and v_3 in both Au+Au and Cu+Cu collisions. The resolution of v_2 shows a peak in mid-central collisions which is consistent with the experimental result [20]. This is because the resolution of v_2 is affected by both of the v_2 signal and the multiplicity used to reconstruct the event plane. While the resolution of v_3 only depends on the multiplicity, and keeps decreasing as the multiplicity drops.

In Fig. 2, v_2 and v_3 are shown as functions of centrality in both Au+Au and Cu+Cu collisions. We can see that v_2 shows strong centrality dependence since it is mainly coming from the elliptic anisotropy in the initial geometry. Unlike v_2, the dependence of v_3 on centrality and system size are much smaller. The trend of v_3 observed is the same as that in Ref [11]. However, the event plane angle Ψ_n in Ref [11] is obtained from the initial parton distribution, which is not observed in the experiment, while in our study it is from the final state particle distribution. The results indicate that the triangular flow is less sensitive to the centrality and system size compared with the elliptic flow. It could be understood as a result of combined effects from initial geometrical fluctuation and collective dynamics which requires the size of bulk to interact among themselves.

It is commonly assumed that the harmonic flow coefficients v_n linearly depends on the ε_n. This assumption is supported by hydrodynamic simulations [10] as long as one probes deformed initial profiles with only a single non-vanishing harmonic eccentricity coefficient. In Fig. 3 and Fig. 4, we investigate the feasibility of this assumption for v_2 and v_3 respectively. The relations between v_n and ε_n are drawn event by event in the two-dimension plots. The black points are the average values of v_n in an selected ε_n bin, and the curves are the connection of points to guide our eyes. The pads in the right down corners are the average values of v_n with smaller scale. In Fig. 3, the v_2 increases with ε_2, which is consistent with the ideal hydrodynamic calculation [21]. While in Fig. 4, the triangular flow v_3 firstly increases with ε_3 up to 0.17, and then decreases. Based on our study, the higher ε_3 bin corresponds to the more peripheral collisions. It is known that v_3 is caused by initial geometrical fluctuation, and built up by the interactions of constituents. The less interactions in the higher ε_3 bin may cause the less converting efficiency from ε_3 to v_3. That could be the reason of decreasing trend of v_3 when ε_3 is larger than 0.17. Both the trend and the value of v_3 show discrepancy to the ideal hydrodynamic calculations [21]. As discussed in Ref. [10], the viscosity causes the decrease of v_3, however, the effects to v_3 versus ε_3 is not shown in the viscous hydrodynamic calculation.

The ratio of elliptic flow to eccentricity v_2/ε_2 gains lots of interests by comparing with the hydrodynamic model [14, 22]. Recently, the behavior of triangular flow v_3 in ideal hydrodynamics is also discussed [10]. In Fig. 5, we study the v_n/ε_n as a function of transverse particle density. From the plot we can see that v_n/ε_n from Au+Au and Cu+Cu are consistent with each other very well. As the transverse particle density increases, v_3/ε_3 rises with smaller value than v_2/ε_2. It implies that as the particle density increases, the initial geometry asymmetry transfers to momentum asymmetry more efficiently while the system expands. Besides, the second order harmonic is more efficient than the third order.

At last, the transverse momentum dependence of v_3 for π, K, p and Λ is also studied in Au+Au and Cu+Cu

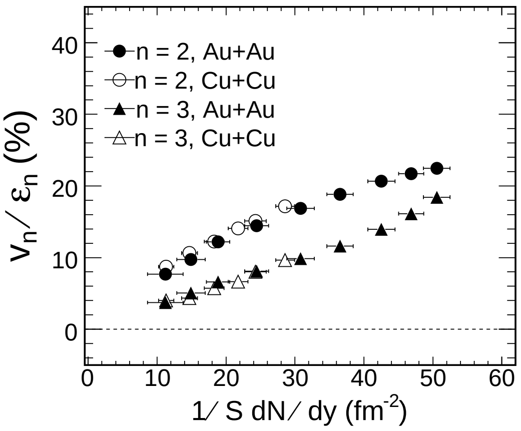

FIG. 5: v_n/ε_n as a function of transverse particle density in both Au+Au and Cu+Cu collisions at $\sqrt{s_{NN}}$=200 GeV in AMPT model.

collisions. In Fig. 6, we can see that v_3 shows quite similar trend to v_2. At low p_T, the mass ordering phenomena is observed. The lighter particles are found with larger v_3. It indicates that although v_3 is driven by ε_3, its transverse momentum dependence is dominated by the hydrodynamics behavior of the system. While when $p_T \geq 1.5$ GeV/c, baryons and mesons are separated into two groups. The p_T dependence of v_3 from identified particles is qualitatively similar to the p_T dependence of v_2 [5, 6]. The v_3 results of identified particles from AMPT model are similar to the STAR preliminary results [23].

V. SUMMARY

In summary, we studied the relation between initial geometry parameter ε_n and anisotropic flow v_n in Au+Au and Cu+Cu collisions using the AMPT Monte-Carlo model. We find that the triangular flow v_3 is less sensitive to the centrality and system size compared with the elliptic flow v_2. The v_2 displays an increasing trend as a function of ε_2, which is qualitatively consistent with hydrodynamic calculation. We found that v_3 shows an increasing trend when ε_3 is less than 0.17, and then decreases beyond $\varepsilon_3 = 0.17$. It may be because of the lower converting efficiency from ε_3 to v_3 in the higher ε_3 bin. This decreasing trend is in contrast to the results of ideal hydrodynamic calculation. Both v_2/ε_2 and v_3/ε_3 increase with the transverse particle density, and the second harmonic asymmetry in the initial geometry seems to transfer to the momentum asymmetry more efficiently than the third harmonic. The triangular flow v_3 of identified particles shows a mass ordering in low p_T and meson-baryon splitting at intermediate p_T in both Au+Au and Cu+Cu collisions which is similar to the p_T dependence of v_2.

VI. ACKNOWLEDGMENTS

We wish to thank Prof. Fuqiang Wang for useful suggestions, and Dr. Kejun Wu for useful discussions on the AMPT model. This work was supported in part by the National Natural Science Foundation of China under grant No. 10775060, 11105060, 11135011, 11147146 and 'the Fundamental Research Funds for the Central Universities', Grant No. HUST: 2011QN195.

---

[1] I. Arsene *et al.* (BRAHMS Collaboration), Nucl. Phys. A **757**, 1 (2005); B. B. Back *et al.* (PHOBOS Collaboration), Nucl. Phys. A **757**, 28 (2005); J. Adams *et al.* (STAR Collaboration), Nucl. Phys. A **757**, 102 (2005); S. S. Adcox *et al.* (PHENIX Collaboration), Nucl. Phys. A **757**, 184 (2005).

[2] J. Adams *et al* (STAR Collaboration), Phys. Rev. Lett. **95** 122301 (2005).

[3] A. M. Poskanzer and S. A. Voloshin, Phys. Rev. C **58**, 1671 (1998).

[4] K. H. Achermann *et al.* (STAR Collaboration), Phys. Rev. Lett. **86**, 402 (2001).

[5] B. I. Abelev *et al* (STAR Collaboration), Phys. Rev. C **77**, 54901 (2008).

[6] B. I. Abelev *et al* (STAR Collaboration), Phys. Rev. C **81**, 044902 (2010).

[7] S. A. Voloshin and A. M. Poskanzer, Phys. Lett. B **474**, 27 (2000). P. F. Kolb, J. Sollfrank and U. W. Heinz, Phys. Rev. C **62**, 054909 (2000).

[8] B. Alver et al., Phys. Rev. Lett. **98**, 242302 (2007); B. Alver et al. PHOBOS Collaboration, Phys. Rev. C **81**, 034915 (2010).

[9] B. Alver and G. Roland, Phys. Rev. C **81**, 054905 (2010); Jun Xu, Che Ming Ko, Phys. Rev. C **83**, 021903 (2011);G.-L. Ma, X.-N. Wang, Phys. Rev. Lett. **106**, 162301 (2011).

[10] B. H. Alver, C. Gombeaud, M. Luzum, and J. Y. Ollitrault, Phys. Rev. C **82**, 034913 (2010).

[11] L.-X. Han *et al.*, arXiv:1105.5415

[12] Z.-W. Lin *et al.*, Phys. Rev. C **59**, 2716 (1999).

[13] B. Alver *et al.* (PHOBOS Collaboration), Phys. Rev. C **77**, 014906 (2008).

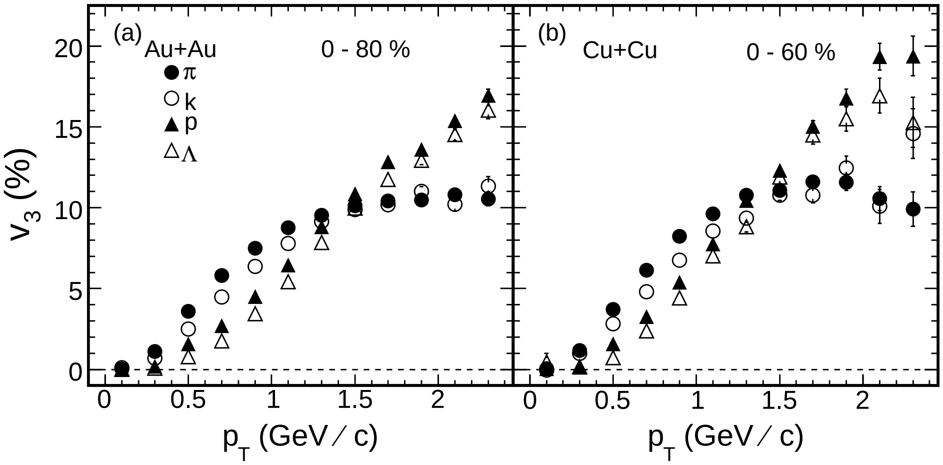

FIG. 6: v_3 as a function of transverse momentum in (a) Au+Au and (b) Cu+Cu collisions at $\sqrt{s_{NN}}$=200 GeV in AMPT model.

[14] J. Y. Ollitrault, Phys. Rev. **D46** 229 (1992).

[15] B. Alver *et al.* (PHOBOS Collaboration), Phys. Rev. Lett. **98**, 242302 (2007).

[16] S. A. Voloshin, A. M. Poskanzer, R. Snellings arXiv:0809.2949 (2008) and Voloshin, Sergei A., Poskanzer, Arthur M., Snellings, Raimond: Collective Phenomena in Non-Central Nuclear Collisions. Stock, R. (ed.). SpringerMaterials - The Landolt-Bornstein Database (http://www.springermaterials.com). Springer-Verlag Berlin Heidelberg, 2010. *DOI* : $10.1007/978-3-642-01539-7_10$

[17] X.-N. Wang, Phys. Rev. **D 43** 104 (1991).

[18] B. Zhang, Comput. Phys. Commun. **109**, 193 (1998).

[19] B.A. Li and C.M. Ko, Phys. Rev. **C 52** 2037 (1995).

[20] J. Adams *et al* (STAR Collaboration), Phys. Rev. C **72**, 14904 (2005).

[21] Z. Qiu and U. Heinz, Phys. Rev. C **84**, 024911 (2005).

[22] H. J. Drescher, A. Dumitru, C. Gombeaud and J. Y. Ollitrault, Phys. Rev. **C76** 024905 (2007).

[23] Y. Pandit for the STAR collaboration, poster, RHIC and AGS Annual Users' Meeting, Upton, NY, Jun. 20-24, 2011.